Journal of Nuclear Materials 404 (2010) 55–59

Contents lists available at ScienceDirect

Journal of Nuclear Materials

journal homepage: www.elsevier.com/locate/jnucmat

The ternary system: Silicon–tantalum–uranium

Peter Rogl [b,*], Henri Noel [a]

[a] Laboratoire de Chimie du Solide et Materiaux, UMR-CNRS 6226, Université de Rennes I, Avenue du Général Leclerc, F-35042 Rennes, Cedex, France
[b] Institute of Physical Chemistry, University of Vienna, A-1090 Wien, Währingerstraße 42, Austria

ARTICLE INFO

Article history:
Received 21 March 2010
Accepted 18 June 2010

ABSTRACT

Phase equilibria in the ternary system Si–Ta–U have been established in an isothermal section at 1000 °C by optical microscopy, electron probe microanalysis and X-ray diffraction. Two novel ternary compounds were observed and were characterised by X-ray powder Rietveld refinement: stoichiometric τ_1-$U_2Ta_3Si_4$ ($U_2Mo_3Si_4$-type, $P2_1/c$; $a = 0.70011(1)$, $b = 0.70046(1)$, $c = 0.68584(1)$ nm, $ß = 109.38(1)$; $R_F = 0.073$, X-ray powder Rietveld refinement) and τ_2-$U_{2-x}Ta_{3+x}Si_4$ at $x \sim 0.30$ ($Sc_2Re_3Si_4$-type = partially ordered Zr_5Si_4-type, $P4_12_12$; $a = b = 0.69717(3)(1)$, $c = 1.28709(4)$ nm; $R_F = 0.056$; X-ray single crystal data). Mutual solubility of U-silicides and Ta-silicides are found to be very small i.e. below about 1 at.%. Due to the equilibrium tie-line Ta_2Si–U(Ta), no compatibility exists between the U-rich silicides U_3Si or U_3Si_2 and tantalum metal.

Single crystals obtained from alloys slowly cooled from liquid (2000 °C), yielded a fully ordered compound $U_2Ta_2Si_3C$ (unique structure type; *Pmna*, $a = 0.68860(1)$; $b = 2.17837(4)$; $c = 0.69707(1)$ nm; $R_{F2} = 0.048$).

1. Introduction

In recent papers we have shown that ternary systems uranium – transition metal – silicon are characterised by the formation of thermodynamically rather stable high temperature compounds $U_2M_3Si_4$, which may adopt three different but closely related structure types with variable stoichiometries: $Sc_2Re_3Si_4$-type (ordered Zr_5Si_4-type, tP36, $U_2Nb_3Si_4$ [1], $U_{2-x}Ti_{3+x}Si_4$ for $0.7 < x < 1.3$ at 1000 °C [2]), $Ce_2Sc_3Si_4$-type (ordered Sm_5Ge_4-type, oP36, $U_{2-x}Nb_{3+x}Si_4$, $x = 0.25$ at 1400 °C [1]) and $U_2Mo_3Si_4$-type (mP18, $U_2Ti_3Si_4$ [2], $U_2Mo_3Si_4$ [3] and $U_2V_3Si_4$ [4]). In case of M = Hf an extended solution $U_xHf_{5-x}Si_4$ of U in binary Hf_5Si_4 (Zr_5Si_4-type) was observed up to $x \leqslant 1.3$ at 1000 °C [5].

In continuation of our research programme on the phase relations and the crystal chemistry in ternary uranium silicide systems, we herein focus on the combination with tantalum, a system on which no information was hitherto presented in literature. As far as the phase equilibria and compatibility of U_3Si_2 with Ta-metal are concerned, the research reported herein is related to low enriched uranium (LEU) proliferation resistant U_3Si_2 dispersion fuels widely used in research reactors [6].

2. Materials and methods

All samples, each of a total amount of about 1 g, were prepared by arc melting the elements under Ti-gettered argon. Platelets or turnings of depleted uranium (claimed purity of 99.9% by Merck, Darmstadt, D), pieces of 6N-silicon (99.9999%) and tantalum foil (99.9%, both from Alfa Ventron, Karlsruhe, D) were used as starting materials. The U-metal was surface cleaned in diluted HNO_3 prior to melting. For homogeneity the samples were re-melted several times; weight losses were checked to be altogether less than 0.5 mass%. A part of each alloy was contained within a small alumina crucible, sealed in an evacuated silica tube and heat-treated at 1000 °C for 200 h and finally quenched by submerging the capsule in cold water. For high-temperature experiments we used a high frequency (HF) furnace (270 kHz) at 1400 °C under argon: arc melted alloys were either slowly cooled from the melt (2000 °C) and/or heat-treated for 15 h in an alumina container within a water-cooled Hukin crucible. DTA was performed in a calibrated Setaram Labsys S60 DTA using alumina crucibles under a stream of argon and heating/cooling rates of 5 K/min. Further details of sample preparation and of the X-ray techniques used (including quantitative Rietveld analyses employing the Fullprof program [7,8]) may be found from our preceding publication on binary uranium silicides [9] or on the ternary system Nb–Si–U [1].

As-cast and annealed samples were investigated by X-ray powder diffraction (XPD), light optical microscopy (LOM) and quantitative electron microprobe analysis (EMPA) on SiC-ground and 1/4 μm diamond paste polished surfaces. A Jeol energy dispersive X-ray microanalyser (EMPA–XMA) was employed for proper identification of the phases operating at an acceleration voltage of 15 kV at 20 nA sample current using the U Mα, Ta Mα and Si Kα radiation. In order to properly account for the overlap of the Ta

---

* Corresponding author. Tel.: +43 1 4277 52456; fax: +43 1 4277 9524.
E-mail address: peter.franz.rogl@univie.ac.at (P. Rogl).

0022-3115/$ - see front matter © 2010 Elsevier B.V. All rights reserved.
doi:10.1016/j.jnucmat.2010.06.030

Mα and Si Kα lines in the EDX system a $TaSi_2$ standard was made. X-ray intensities were corrected for ZAF effects.

Single crystals were mechanically isolated from a crushed as cast alloy with nominal composition $U_{11}Ta_{44}Si_{45}$ (for $U_{2-x}Ta_{3+x}Si_4$) and $U_{35}Ta_{25}Si_{40}$ (for $U_2Ta_2Si_3C$), respectively, where the latter was re-melted after arc melting under argon in a Hukin crucible of a HF furnace at ~2000 °C and slowly cooled (2 h) to 1000 °C. X-ray intensity data were collected on a four-circle Nonius Kappa diffractometer equipped with a CCD area detector employing graphite monochromated Mo Kα radiation ($\lambda = 0.071073$ nm). Orientation matrix and unit cell parameters were derived using the program DENZO [10]. Absorption correction was applied approximating the irregular crystal shape by 21 crystallographic planes. The structures were solved by direct methods and refined with the aid of the SHELXL-97 and SHELXS-97 program [11].

3. Results and discussion

3.1. Binary boundary systems

Both boundary systems, Ta–U and Si–Ta, have been accepted from the compilation of binary alloy phase diagrams [12]. The U–Si system used herein is from a reinvestigation by the authors [9,13,14], but the uranium-rich part of the diagram up to 4 at.% Si is taken from Straatmann and Neumann [15] and Holleck and Kleykamp [16]. Crystallographic data of the boundary phases [16,17] are listed in Table 1.

3.2. Phase relations at 1000 °C

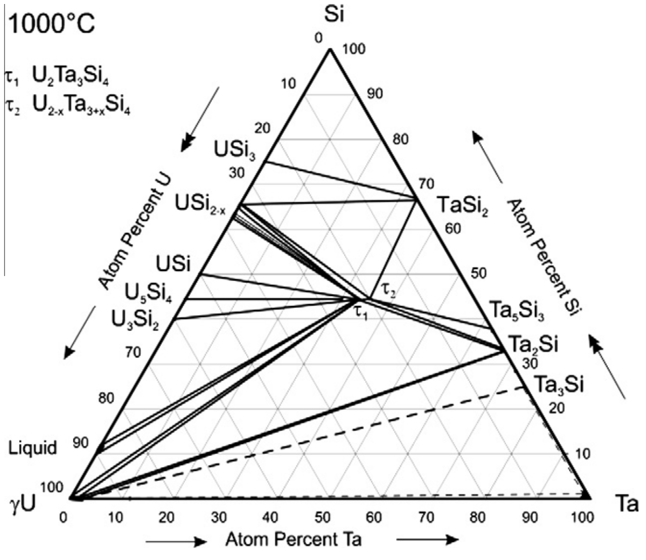

Fig. 1. System Si–Ta–U; isothermal section at 1000 °C.

Phase relations within the Si–Ta–U ternary system were established for the isothermal section at 1000 °C, revealing two hitherto unknown ternary compounds τ_1 and τ_2 close to the composition $U_2Ta_3Si_4$ (Fig. 1). From optical microscopy, from variation of lattice parameters and particularly from EMP-analyses, these phases are observed close to each other without a significant homogeneous region. Whereas τ_1-$U_2Ta_3Si_4$ seems to exist at the stoichiometric composition, τ_2-$U_{2-x}Ta_{3+x}Si_4$ appears at a composition slightly richer in Ta ($x \sim 0.30$). The ternary phases, however, do not melt congruently and form at high temperature via a presumably peritectic reaction $L + U_3Si_5 + Ta_2Si = U_2Ta_3Si_4$ as indicated from the microstructures in Fig. 2. Due to the rather high thermodynamic stability of Ta_2Si and the τ_1 and τ_2 phases, tie-lines exist between these compounds and U(Ta) and as a consequence no compatibility exists for the join U_3Si_2–Ta(U). Mutual solubility of U-silicides and Ta-silicides in alloys annealed at 1000 °C are found to be very small

Table 1
Crystallographic data of binary boundary and ternary phases of the system Si–Ta–U.

Phase	Pearson symbol	Space group	Proto type	Lattice parameter in nm			Remarks	References
				a	*b*	*c*		
γU	cI2	$Im\bar{3}m$	W	0.3524			1132.3–774.8 °C	[12,16,17]
				0.35335			at 787 °C	
βU	tP30	$P4_2/mnm$	βU	1.0759		0.5656	774.8–667.7 °C	[12,16,17]
				1.07589		0.56531	at 682 °C	
αU	oC4	Cmcm	αU	0.28537	0.58695	0.49548	<667.7 °C	[12,16]
Ta	cI2	$Im\bar{3}m$	W	0.330256			<3020 °C at 299 K	[12,17]
Si	cF8	$Fd\bar{3}m$	Cdiamond	0.543065			<1414 °C	[12]
Ta_3Si	tP32	$P4_2/n$	Ti_3P	1.0184		0.5183	<2340 °C	[12,17]
Ta_2Si	tI12	I4/mcm	$CuAl_2$	0.6172		0.5050	<2440 °C	[12,17]
βTa_5Si_3	tI32	I4/mcm	W_5Si_3	0.9892		0.5042	2550–2160 °C	[12,17]
αTa_5Si_3	tI32	I4/mcm	Cr_5B_3	0.6517		1.1872	<2160 °C	[12,17]
$TaSi_2$	hP9	$P6_222$	$CrSi_2$	0.4782	–	0.6565	<2040 °C	[12,17]
γU_3Si	cP4	$Pm\bar{3}m$	Cu_3Au	0.4346			930–759 °C	[12,21]
βU_3Si	tI16	I4/mcm	βU_3Si	0.60328		0.86907	762 to −153 °C	[15,17]
αU_3Si	oF32	Fmmm	αU_3Si	0.8654	0.8549	0.8523	<−153 °C, at −193 °C	[15,17]
U_3Si_2	tP10	$P4/mbm$	U_3Si_2	0.73299		0.39004	<1665 °C	[12,17]
U_5Si_4	hP36	$P6/mmm$	$U_{20}Si_{16}C_3$	1.0467		0.7835		[14]
USi	tI38	I4/mmm	USi	1.058		2.431	<1580 °C	[13]
USi[a]	oP8	Pnma	FeB	0.7585	0.3903	0.5663		[22]
U_3Si_5	hP3	$P6/mmm$	AlB_2	0.3843		0.4069	<1770 °C	[12]
U_3Si_5(o1)	oP6	Pmmm	Dist. AlB_2	0.3869	0.6660	0.4073	At 63 at.%Si	[9]
U_3Si_5(o2)	oP6	Pmmm	Dist. AlB_2	0.3893	0.6717	0.4042	At ~63 at.%Si	[9]
USi_{2-z}	oI12	Imma	Def. $GdSi_2$	0.3953	0.3929	1.3656	At 64 at.% Si	[9]
USi_{2-z}	tI12	$I4_1/amd$	Def. $ThSi_2$	0.39423		1.3712	<1710 °C, at 65 at.%Si	[9,12]
USi_2	tI12	$I4_1/amd$	$ThSi_2$	0.3922		1.4154	<450 °C	[12,17]
USi_3	cP4	$Pm\bar{3}m$	Cu_3Au	0.4060			<1510 °C	[12]
τ_1-$U_2Ta_3Si_4$	mP18	$P2_1/c$	$U_2Mo_3Si_4$	0.70011(1)	0.70046(1)	0.68584(1)	$\beta = 109.38(1)°$	This work
τ_2-$U_{2-x}Ta_{3+x}Si_4$	tP36	$P4_12_12$	$Sc_2Re_3Si_4$	0.69717(3)	0.69717(3)	1.28709(4)	–	This work

[a] Probably oxygen stabilized [9].

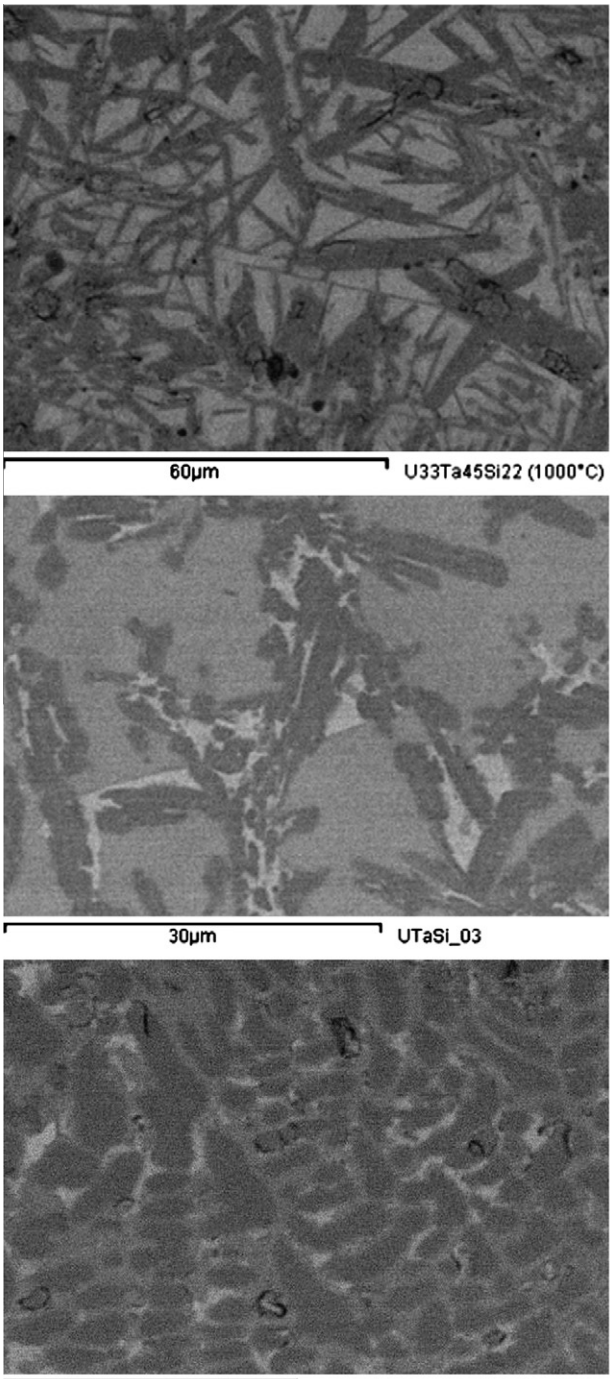

Fig. 2. EMPA-backscatter images. Upper panel: $U_{33}Ta_{45}Si_{22}$, annealed at 1000 °C; dark needles $U_{0.2}Ta_{66.3}Si_{33.5}$ (Ta_2Si), bright matrix $U_{98.4}Ta_{0.9}Si_{0.7}$ (U(Ta)). Middle panel: $U_{60}Ta_{10}Si_{30}$, as cast; grey precipitates $U_{60.2}Ta_{0.06}Si_{39.2}$ (U_3Si_2); dark crystals $U_{22.1}Ta_{33.3}Si_{44.6}$ (τ_1); bright regions $U_{98}Ta_{1.7}Si_{0.3}$ (U(Ta)). Lower panel: $U_{20}Ta_{45}Si_{35}$, annealed at 1000 °C; diffuse dark dendrites $U_{0.03}Ta_{65}Si_{35}$ (Ta_2Si), grey peritectic seams $U_{19}Ta_{36.4}Si_{44.6}$ (τ_2); bright regions $U_{98}Ta_{1.6}Si_{0.4}$ (U(Ta)).

i.e. below about 0.6 at.%. In order to check on the possible formation of a ternary compound "$U_4Ta(Ta_xSi_{1-x})Si_2$" with W_5Si_3-type as well as on the maximum solubility of Ta in U_3Si_2, two samples, $U_{60}Ta_{10}Si_{30}$ and $U_{50}Ta_{10}Si_{40}$, were investigated. EMPA data undoubtedly proved the absence of a ternary W_5Si_3-type compound as well as proved a negligible solubility of Ta in U_3Si_2. Furthermore the phase equilibrium $U_3Si_2 + \tau_1$ was confirmed as well as τ_1 connecting with U(Ta) (see microstructures in Fig. 2).

Table 2
Crystallographic data of the ternary compound τ_1-$U_2Ta_3Si_4$; $U_2Mo_3Si_4$-type, $P2_1/c - C_{2h}^5$; no. 14, origin at $\overline{1}$, $Z = 2$. X-ray powder Rietveld refinement $a = 0.70011(1)$, $b = 0.70046(1)$, $c = 0.68584(1)$ nm, $\beta = 109.38(1)$; $R_F = 0.073$.

Atom	Site	x	y	z	B[a]	Occupation
U1	4e	0.6899(5)	0.3303(5)	0.0697(4)	0.20(6)	1.01(1)
Ta1	2d	0	0	0	0.21(4)	1.01(3)
Ta2	4e	0.2511(7)	0.3257(9)	0.2550(8)	0.38(5)	1.0(−)
Si1	4e	0.4098(11)	0.0457(12)	0.1314(10)	0.62(5)	1.0(1)
Si2	4e	0.0037(12)	0.1332(14)	0.3673(13)	0.54(5)	1.0(1)

[a] Data in 100 nm^2 (=$Å^2$).

3.2.1. The phases $U_2Ta_3Si_4$ with the $U_2Mo_3Si_4$-type and $U_{2-x}Ta_{3+x}Si_4$, $x = 0.30$, with the $Sc_2Re_3Si_4$-type (partially ordered Zr_5Si_4-type)

It was impossible to obtain single-phase X-ray powder patterns of each of the two ternary phases τ_1-$U_2Ta_3Si_4$ and τ_2-$U_{2-x}Ta_{3+x}Si_4$ although alloys with varying compositions were re-melted in the HF furnace under argon and slowly cooled, or alternatively annealed at 1400 °C and quenched. Depending on composition the X-ray powder spectra showed different amounts of the two phases und were successfully indexed on the basis of a phase mixture of: (a) a primitive monoclinic cell and (b) a primitive tetragonal unit cell (see Tables 1–3). Extinctions for the monoclinic phase: $(0\,k\,0)$ extinct for $k = 2n + 1$ and $(h\,0\,l)$ for $l = 2n + 1$ prompted a space group symmetry $P2_1/c$ indicating isotypism with the $U_2Mo_3Si_4$-type [18]. Extinctions for τ_2 were observed only for screw axes 4_1 and 2_1: $(0\,0\,l)$ and $(h\,0\,0)$ extinct for $l = 4n + 1$ and $h = 2n + 1$, respectively, and thus are compatible with $P4_12_12$ as the highest symmetric space group. The chemical formula, the unit cell dimensions, crystal symmetry and X-ray intensities strongly suggest isotypism with the $Sc_2Re_3Si_4$-type [19]. Whereas no suitable single crystals could be obtained for τ_1-$U_2Ta_3Si_4$, a single crystal fragment crushed from the cast alloy with nominal composition $U_{11}Ta_{44}Si_{45}$ turned out to be tetragonal with $P4_12_12$ symmetry. Single crystal X-ray intensity data refinement prompted isotypism with the Zr_5Si_4-parent type close to the ordered variant: $Sc_2Re_3Si_4$-type. Crystal structure analysis unambiguously revealed a small random occupation of (6.80 U + 1.20 Ta) atoms in the 8*b* site yielding a non-stoichiometric composition at $x \sim 0.30$. Structure parameters and results of the refinement for $U_{2-x}Ta_{3+x}Si_4$ ($x \sim 0.30$) which converged to $R_{F^2} = 0.056$ with residual electron densities smaller than ± 5000 e^-/nm^3, are summarized in Table 3.

Starting from the atom order and the atom parameter set of the two structure types, a full matrix – full profile Rietveld refinement of a Siemens D5000 flat specimen X-ray powder intensity recording satisfactorily converged at reasonably low residual values $R_F = 0.073$ for τ_1 and $R_F = 0.064$ for τ_2 (confirming the single crystal data for τ_2). Occupancies have been refined for all atom sites revealing no deviation from the atom distribution given except for one uranium position (8*b* site) in τ_2-$U_{2-x}Ta_{3+x}Si_4$, confirming the mixed occupation of (6.8 U + 1.2 Ta) atoms. Due to the usually strong correlation between occupational and thermal parameters, the isotropic temperature coefficients were individually analysed and kept constant throughout the powder refinement. The final structure and profile parameters and the reliability values obtained from the least squares refinements are presented in Tables 2 and 3 and were made consistent with a standardised setting of the atom positions employing the program *Structure Tidy* [20].

3.3. Crystal structure of $U_2Ta_2Si_3C$

During the course of the investigation arc melted samples, which were re-melted under argon in a high frequency Hukin crucible and slowly cooled from liquid (2000 °C) to 1000 °C during 2 h, were highly crystalline. Single crystals were obtained via mechan-

Table 3
Crystallographic data of the ternary compound τ_2-$U_{2-x}Ta_{3+x}Si_4$; $Sc_2Re_3Si_4$-type, $P4_12_12 - D_4^4$; no. 92, origin at 2_12; $Z = 4$; X-ray single crystal refinement [a]. $a = b = 0.69717(3)$, $c = 1.28709(4)$ nm; $R_{F2} = 0.057$ for 635 $F_o > 4\sigma(F_o)$ of 711 reflections (total 7894); GOF = 1.062.

Atom	Site	x	y	z	$U_{eq.}$[b]	Occupation
U1 + Ta1	8e	0.5001(2)	0.1635(2)	0.2189(1)	0.0111(4)	0.85(1)U + 0.15Ta
Ta2	8d	0.0015(2)	0.1569(2)	0.1257(1)	0.0111(4)	1.0
Ta3	4e	0.3307(2)	0.3307(2)	0.0	0.0109(5)	1.0
Si1	8e	0.130(1)	0.205(1)	0.3177(6)	0.012(2)	1.0
Si2	8e	0.206(1)	0.457(1)	0.1855(7)	0.012(2)	1.0

[a] EXTI (Zachariasen) = 0.00034(2). Residual electron densities: max 4790, min −5150 e⁻/nm³.
[b] Data in 100 nm² (=Å²).

ical fragmentation from the alloy with nominal composition $U_{35}Ta_{25}Si_{40}$. The structure model, obtained by direct methods, satisfactorily refined to $R_{F2} = 0.048$ yielding a fully ordered metal arrangement with a chemical formula $U_2Ta_2Si_3$. At this stage significant residual densities were located in the centers of octahedra $[U_4Ta_2]$, which seemed to correspond to the scattering power of carbon atoms. Refinement with C atoms within the octahedra slightly reduced the R-value to 0.044 and prompted: (i) a stable isotropic C-atom displacement parameter and (ii) interatomic distances $d_{Ta-C} = 0.2143$ nm, $0.2539 < d_{C-U} < 0.2573$ nm, well corresponding to the sum of atom radii of U, Ta and C atoms. Alternatively, a defect position with oxygen or nitrogen can be envisaged. Table 4 summarizes the results of the structure refinement. Except for $d_{U1-U1} = 0.3448$ nm, there are no direct U–U contacts below 0.38 nm. Fig. 3 shows the crystal structure of $U_2Ta_2Si_3C$ in three-dimensional view revealing the $C[U_4Ta_2]$ octahedra as well as a row of triangular metal prisms. These prisms with their rectangular faces, capped by two metal atoms and one silicon,

Table 4
X-ray single crystal data for $U_2Ta_2Si_3C$.[a]

Parameter/temperature	$U_2Ta_2Si_3C$	Interatomic distances (standard deviations < 0.00005)	
Formula from refinement	$U_2Ta_2Si_3C$		
Structure type	$U_2Ta_2Si_3C$	U1–1 Si2 0.28324	Ta2–1 Si2 0.25862
Space group	Pmna; No. 53	1 Si3 0.28645	1 Si1 0.26101
Crystal size	54 × 70 × 84 μm³	1 Si3 0.29171	1 Si1 0.26583
Lattice parameters: a; b; c (nm)	0.68860(1); 2.17837(4); 0.69707(1)	1 Si2 0.29207	1 Si2 0.26640
μ_{abs} (mm^{-1}); $\rho_{X\text{-}ray}$ (Mg m^{-3})	103.92; 11.783	1 Si2 0.29359	1 Si2 0.26817
Data collection, 2Θ (°)	$5.82 \leqslant 2\Theta \leqslant 84.13$; 150 s/frame	1 Si1 0.29395	1 Si3 0.26890
Reflections in refinement	2953 $F_0 \geqslant 4\sigma(F_0)$ of 3712	1 Si2 0.30422	1 Ta1 0.30361
Mosaicity	<0.37	1 Ta1 0.32933	1 Ta1 0.30389
Number of variables	72	1 Ta1 0.32960	1 U1 0.33116
$R_{F2} = \Sigma\lvert F_0^2 - F_c^2\rvert/\Sigma F_0^2$	0.044	1 Ta2 0.33116	1 U1 0.33661
R_{Int}	0.092	1 Ta2 0.34480	1 U1 0.36486
wR2	0.107	1 U1 0.34480	
GOF	1.086		Si1–1 Si3 0.24733
Extinction (Zachariasen)	0.00091(5)	U2–1 C 0.25394	1 Ta2 0.26102
		1 C 0.25616	1 Ta2 0.26583
U1 in 8d (x, y, z); occ. = 1.00(1)	x = 0.00153(4), y = 0.05775(1); z = 0.66902(4)	2 Si1 0.28668	1 Ta1 0.27392
U_{11}; U_{22}; U_{33} (in 10^2 nm^2)	0.0061(1), 0.0036(1), 0.0055(1)	2 Si1 0.29739	1 Ta1 0.27509
		2 Si3 0.30195	1 U2 0.28668
U2 in 4c (x, ¼, z); occ. = 1.00(1)	x = 0.34725(6), z = 0.32461(6)	2 Ta1 0.33108	1 U1 0.29395
U_{11}; U_{22}; U_{33} (in 10^2 nm^2)	0.0066(1), 0.00340(1), 0.0057(1)	1 Ta1 0.33494	1 U2 0.29739
U3 in 4c (x, ¼, z); occ. = 1.00(1)	x = 0.49349(5), z = 0.82370(6)	U3–1 C 0.25431	Si2–1 Si2 0.25827
U_{11}; U_{22}; U_{33} (in 10^2 nm^2)	0.0065(1); 0.0033(1); 0.0060(2)	1 C 0.25731	1 Ta2 0.25862
		2 Si3 0.28638	1 Ta2 0.26640
Ta1 in 8d (x, y, z); occ.=1.00(1)	x = 0.16803(4), y = 0.15165(1); z = 0.00063(4)	2 Si1 0.29833	1 Ta2 0.26817
U_{11}; U_{22}; U_{33} (in 10^2 nm^2)	0.0059(1), 0.0039(1), 0.0053(1)	2 Si3 0.30099	1 Ta1 0.27874
		2 Ta1 0.33379	1 U1 0.28324
Ta2 in 8d (x, y, z); occ. = 1.00(1)	x = 0.34012(4), y = 0.07667(1), z = 0.32594(4)	2 Ta1 0.33393	1 U1 0.29207
U_{11}; U_{22}; U_{33} (in 10^2 nm^2)	0.0068(1), 0.0038(1,) 0.0054(1)		1 U1 0.29359
		Ta1–1 C 0.21433	1 U1 0.30422
Si1 in 8d (x, y, z); occ. = 1.00(1)	x = 0.0455(4), y = 0.1538(1), z = 0.3762(4)	1 Si3 0.26995	
U_{11}; U_{22}; U_{33} (in 10^2 nm^2)	0.0079(9), 0.0040(9), 0.0059(9)	1 Si1 0.27392	Si3–1 Si1 0.24733
		1 Si3 0.27490	1 Ta2 0.26890
Si2 in 8d (x, y, z); occ. = 1.00(1)	x = 0.1657(3), y = 0.0244(1), z = 0.0409(4)	1 Si1 0.27509	1 Ta1 0.26995
U_{11}; U_{22}; U_{33} (in 10^2 nm^2)	0.0071(9), 0.0054(9), 0.0057(8)	1 Si2 0.27874	1 Ta1 0.27490
		1 Ta2 0.30361	1 U3 0.28638
Si3 in 8d (x, y, z); occ. = 1.00(1)	x = 0.2016(3), y = 0.6523(1), z = 0.1279(4)	1 Ta2 0.30389	1 U1 0.28645
U_{11}; U_{22}; U_{33} (in 10^2 nm^2)	0.0076(9), 0.0051(9), 0.0049(8)	1 U1 0.32933	1 U1 0.29171
		1 U1 0.32960	1 U3 0.30099
C in 4c (x, ¼, z); occ.=1.02(2)	x = 0.171(1), z = 0.001(1)	1 U2 0.33108	1 U2 0.30195
U_{iso} (in 10^2 nm^2)	0.012(2)	1 U3 0.33379	C–2 Ta1 0.21433
			1 U2 0.25394
Residual density; max; min	11.7; −7.6 e⁻/Å³		1 U3 0.25431
			1 U2 0.25616
			1 U3 0.25731

[a] Standardised with program Structure Tidy [20].

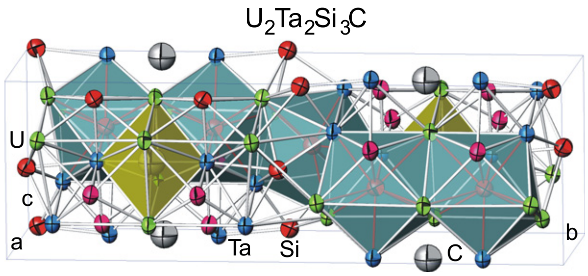

Fig. 3. Crystal structure of $U_2Ta_2Si_3C$ in three-dimensional view. Coordination polyhedra around carbon atoms (octahedra) and around silicon atoms (tetrakaidecahedra = trigonal prisms with rectangular faces capped by three atoms) are outlined.

are centered by Si-atoms: Si1[U_4Ta_4Si], Si2[U_4Ta_4Si] and Si3[U_5Ta_3Si]. X-ray powder patterns of this structure were not encountered in the alloys used for the phase diagram study.

4. Summary

Phase equilibria in the ternary system Si–Ta–U have been established in an isothermal section at 1000 °C. Two novel ternary compounds were observed and were characterised by X-ray data refinement: stoichiometric τ_1-$U_2Ta_3Si_4$ ($U_2Mo_3Si_4$-type) and τ_2-$U_{2-x}Ta_{3+x}Si_4$ (Zr_5Si_4-type) at $x \sim 0.30$. Mutual solubility of U-silicides and Ta-silicides are found to be very small i.e. below about 1 at.%. Single crystals obtained from alloys slowly cooled from liquid (2000 °C), yielded a fully ordered compound $U_2Ta_2Si_3C$ (unique structure type; *Pmna*, $a = 0.68860(1)$; $b = 2.17837(4)$; $c = 0.69707(1)$ nm; $R_{F2} = 0.048$; from X-ray single crystal data).

Acknowledgement

The authors are grateful to the French-Austrian Bilateral Scientific Technical Exchange Programme “Amadee”, Project FR10/2008.

References

[1] T. LeBihan, H. Noël, P. Rogl, J. Nucl. Mater. 277 (2000) 82.
[2] F. Weitzer, H. Noël, P. Rogl, J. Alloys Comp. 350 (2003) 155.
[3] P. Rogl, T. LeBihan, H. Noël, J. Nucl. Mater. 288 (2001) 66.
[4] H. Noël, P. Rogl, J. Nucl. Mater., submitted for publication.
[5] F. Weitzer, P. Rogl, H. Noël, J. Alloys Comp. 387 (2005) 246.
[6] US Nuclear Regulatory Commission Report, NUREG-1313, July 1988.
[7] J. Rodriguez-Carvajal, Physica B 192 (1993) 55.
[8] T. Roisnel, J. Rodriguez-Carvajal, WinPLOTR, a tool to plot powder diffraction patterns. Laboratoire Leon Brillouin (CEA-CNRS) France, 1998.
[9] K. Remschnig, T. LeBihan, H. Noël, P. Rogl, J. Solid State Chem. 97 (1992) 391.
[10] Nonius Kappa CCD Program Package COLLECT, DENZO, SCALEPACK, SORTAV, Nonius Delft, The Netherlands, 1998.
[11] G.M. Sheldrick, SHELXL-97, Program for Crystal Structure Refinement. University of Göttingen, Germany; Windows Version by McArdle, Natl. Univ. Ireland, Galway, 1997.
[12] T.B. Massalski, in: Binary Alloy Phase Diagrams, second ed., ASM International, Materials Park, OH, 1990.
[13] T. LeBihan, Thesis, Université de Rennes, France, 1993, pp. 1–194.
[14] H. Noël, V. Queneau, J.P. Durand, P. Colomb, in: Abstract of a Paper at Int. Conf. on Strongly Correlated Electron Systems – SCES98, 15–18 Juillet, Paris, 1998, p. 92.
[15] J.A. Straatmann, N.F. Neumann, Equilibrium Structure in the High Uranium Silicon Alloy System, USAEC Report MCW-1486, Malinckrodt Chemical Works, October 23, 1964, cited in Reactor Materials, vol. 8(2), 1965, pp. 57-73.
[16] H. Holleck, H. Kleykamp, in: Gmelin Handbook of Inorganic Chemistry, Uranium, vol. C12 (Suppl), Springer, New York, 1987, pp 1–279.
[17] P. Villars, L.D. Calvert, in: Pearson’s Handbook of Crystallographic Data for Intermetallic Phases, second ed., ASM International, Materials Park, Ohio, 1991.
[18] M. Sikiritsa, L.G. Akselrud, Y.P. Yarmolyuk, The Crystal Structure of the Compound $U_2Mo_3Si_4$, in: Abstracts of the 3rd All-Union Conference on the Crystallochemistry of Intermetallic Compounds (in Russian), Vishcha Skhola, L’viv, 1978, p. 11.
[19] V.K. Pecharskii, O.I. Bodak, E.I. Gladyshevskii, Dokl. Akad. Nauk Ukr. RSR A40 (1978) 755–759.
[20] E. Parthé, L. Gelato, B. Chabot, M. Penzo, K. Cenzual, R. Gladyshevskii, TYPIX Standardized Data and Crystal Chemical Characterization of Inorganic Structure Types, Springer, Berlin, Heidelberg, 1994.
[21] Z.M. Alekseeva, J. Nucl. Mater. 186 (1992) 294.
[22] W.H. Zachariasen, Acta Crystallogr. 2 (1949) 94.